

Triboelectric Nanogenerators Enhanced by Metal-Organic Framework for Sustainable Power Generation and Air Mouse Technology

Zahir Abbas ^{a, +}, Monunith Anithkumar ^{b, +}, Asokan Poorani Sathya Prasanna ^b, Nissar Hussain ^a, Sang-Jae Kim ^{*, b,c}, Shaikh M. Mobin ^{*, a, d}

^a Department of Chemistry, Indian Institute of Technology Indore, Simrol, Khandwa Road, Indore 453552, India

^b Nanomaterials & System Laboratory, Major of Mechatronics Engineering, Faculty of Applied Energy System, Jeju National University, Jeju 63243, Republic of Korea

^c R&D centre for Energy New Industry, Jeju National University, Jeju 63243, Republic of Korea

^d Center for Advanced Electronics (CAE), Indian Institute of Technology, Indore, Simrol, Khandwa Road, Indore 453552, India.

***Corresponding author**

Email: xray@iiti.ac.in (Shaikh M. Mobin), kimsangj@jejunu.ac.kr (Sang-Jae Kim)

Equal contribution

[+] These authors contributed equally to this work

Materials characterizations

Materials:

2 aminotetraphalic acid and azo pyridine were procured from Sigma Aldrich, and methanol, and acetone was procured from SRL chemicals. Deionized water was used throughout the study. All the materials were utilized as such without any further purification.

Physical Measurements

The Single crystal data were collected by using graphite-monochromated Mo K α radiation ($\lambda\alpha = 0.71073 \text{ \AA}$). Thermogravimetric analysis (TGA) was recorded with a METTLER TOLEDO (TGA/DSC1) system through STARe software by a heating rate of 10 °C/min in an N₂ atmosphere up to 800 °C. For the Powder X-ray diffraction (PXRD) analysis, Cu K α (0.154 nm) monochromatic radiation was used with a Rigaku Smart Lab X-ray diffractometer. The morphologies were investigated by a Supra55 Zeiss field emission scanning electron microscope (FESEM). Brunauer–Emmett–Teller (BET) surface area and Barrett–Joyner–Halenda (BJH) distribution determinations were conducted on an Autosorb iQ (Quantachrome Instruments, version 1.11). The output performance of the device, load matching analysis, stability, and commercial capacitor charging study were measured using a Keithley 6514 electrometer.

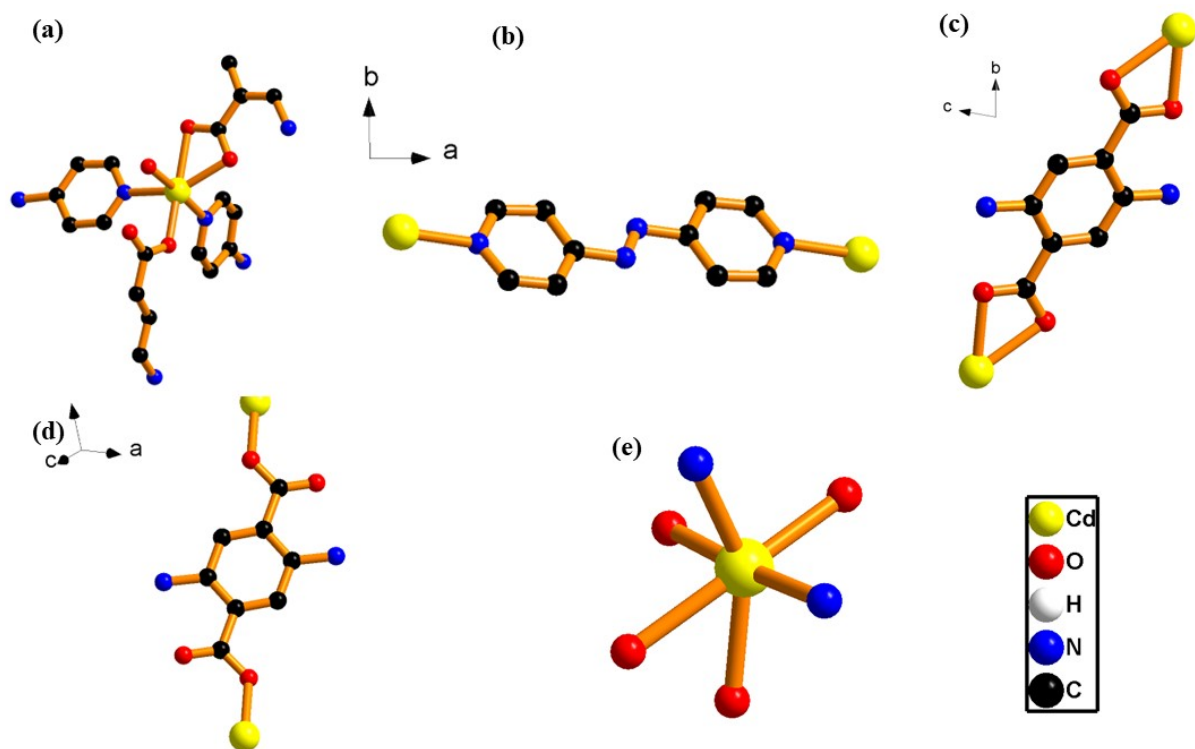


Fig S1. (a)The asymmetric unit of Cd-MOF (b) AzPy binding mode (c-d) 2ATA-binding mode (e) metal binding mode.

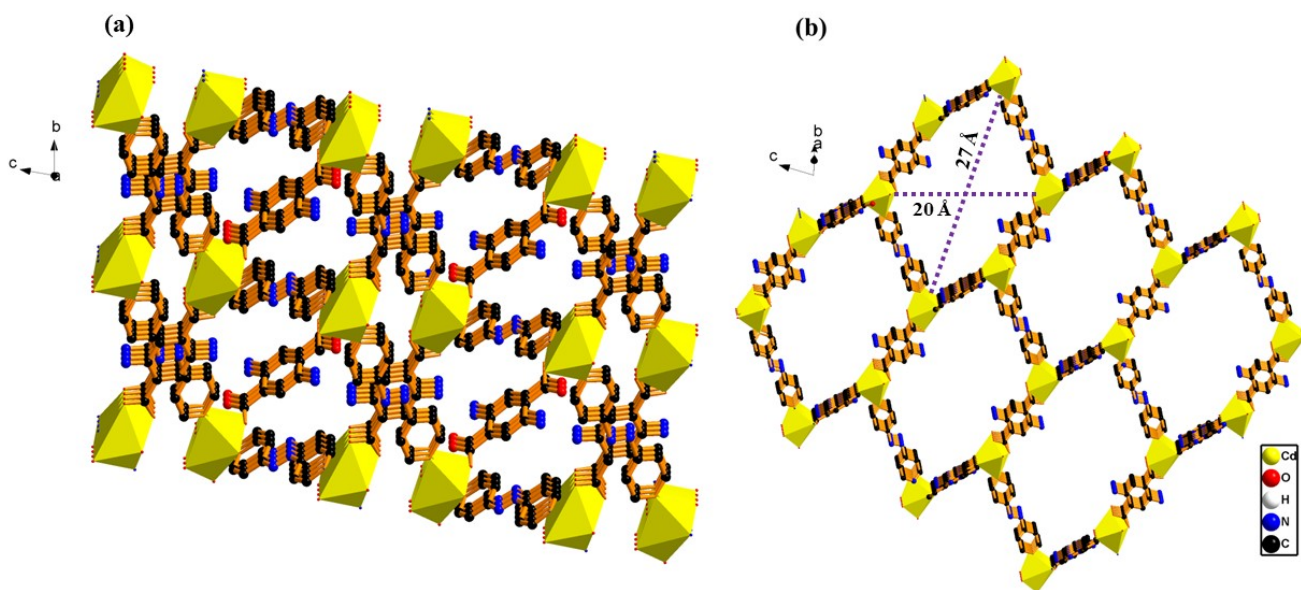


Fig S2. (a) 2D network of Cd-MOF along a-axis with polyhedra (b) Porous nature of Cd-MOF having metal-metal pore aperture.

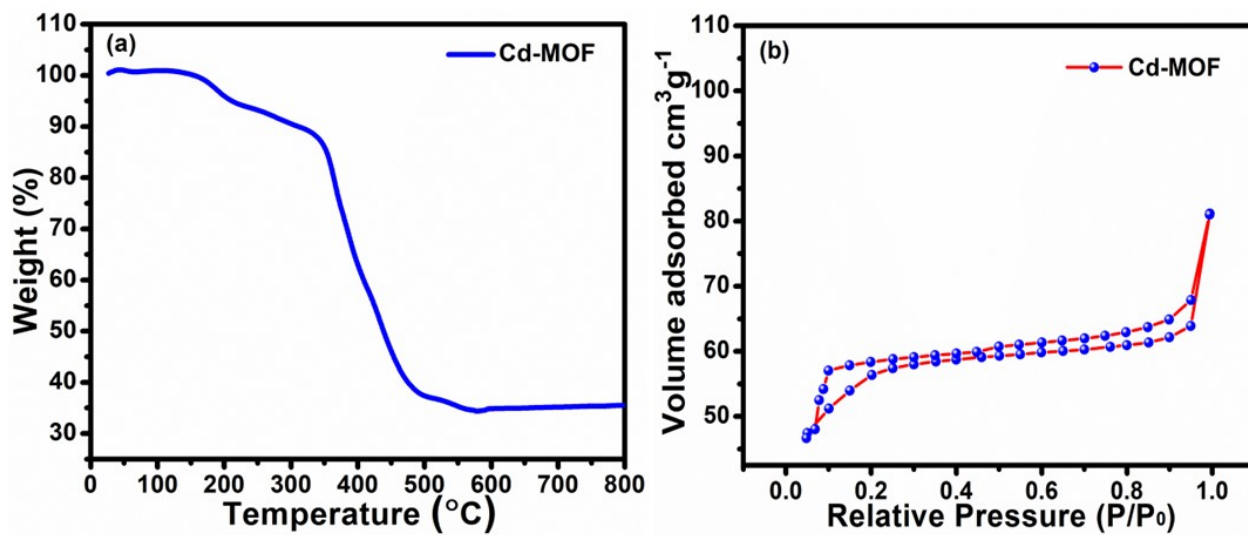


Fig S3. (a) Thermogravimetric analysis curve of Cd-MOF (b) BET analysis of Cd-MOF.

Sample Details

Sample Name: CD-MOF 2

SOP Name: mansettings.nano

General Notes:

File Name: Since Dec 2021.dts

Dispersant Name: Water

Record Number: 1251

Dispersant RI: 1.330

Date and Time: Monday, September 26, 2022 5:2...

Viscosity (cP): 0.8872

Dispersant Dielectric Constant: 78.5

System

Temperature (°C): 25.0

Zeta Runs: 12

Count Rate (kcps): 181.6

Measurement Position (mm): 2.00

Cell Description: Clear disposable zeta cell

Attenuator: 4

Results

	Mean (mV)	Area (%)	St Dev (mV)
Zeta Potential (mV): -16.2	Peak 1: -16.2	100.0	4.71
Zeta Deviation (mV): 4.71	Peak 2: 0.00	0.0	0.00
Conductivity (mS/cm): 0.0900	Peak 3: 0.00	0.0	0.00

Result quality : **Good**

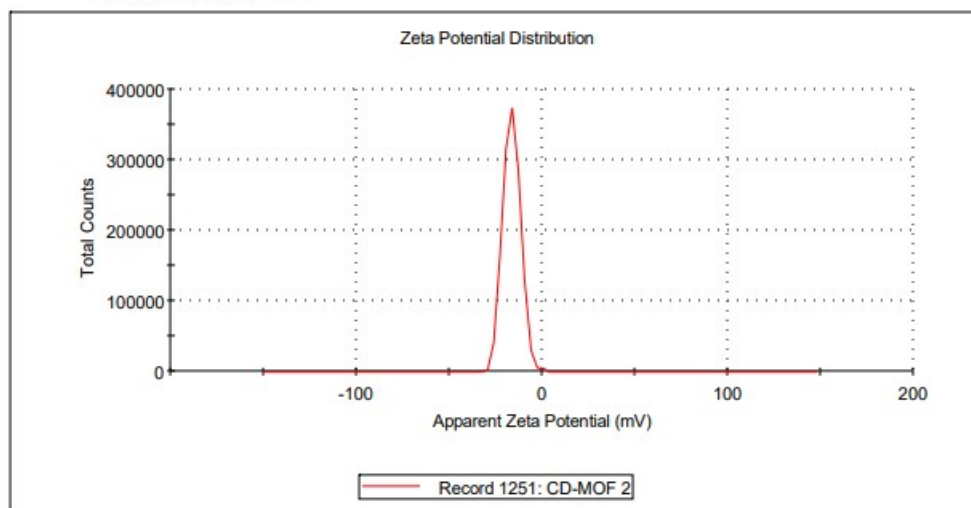


Fig S4. Zeta potential summary and Zeta potential plot of Cd-MOF.

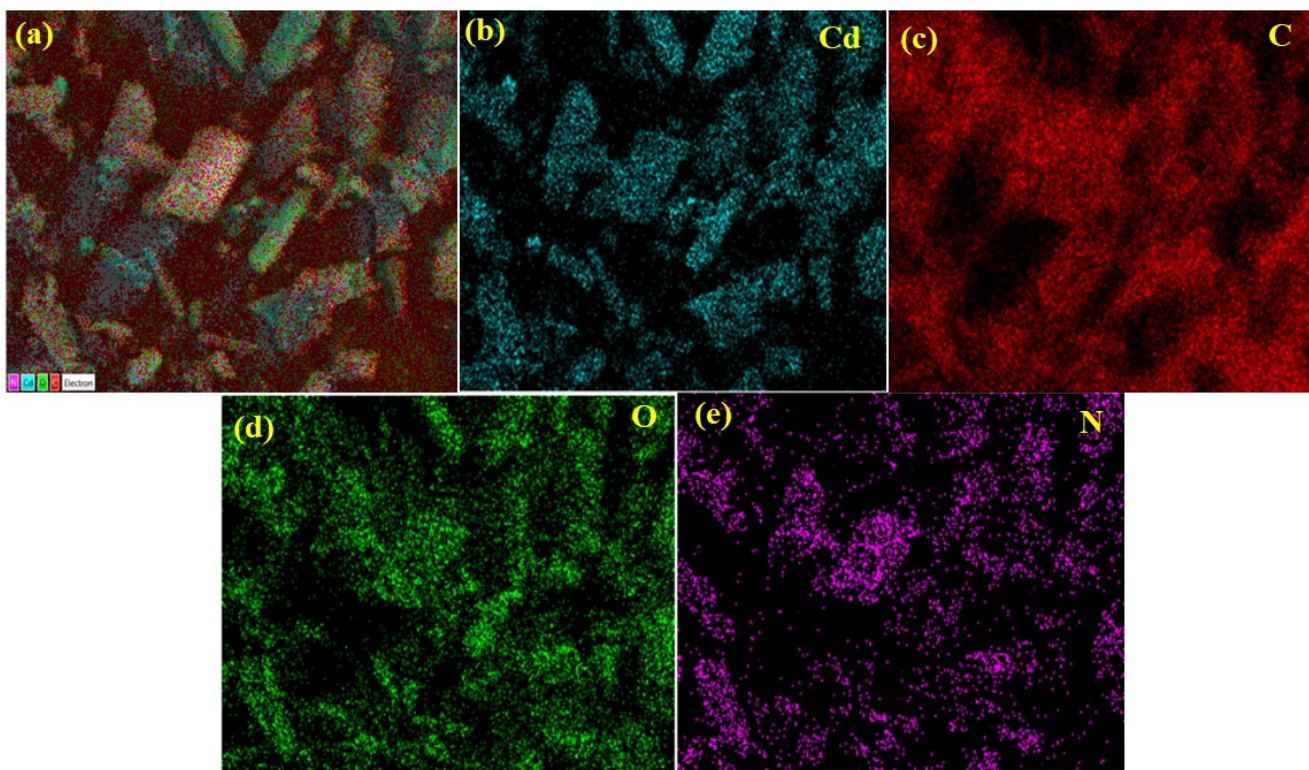


Fig S5. EDS mapping of Cd-MOF (a) SEM (b) Cd (c) C (d) O (e) N.

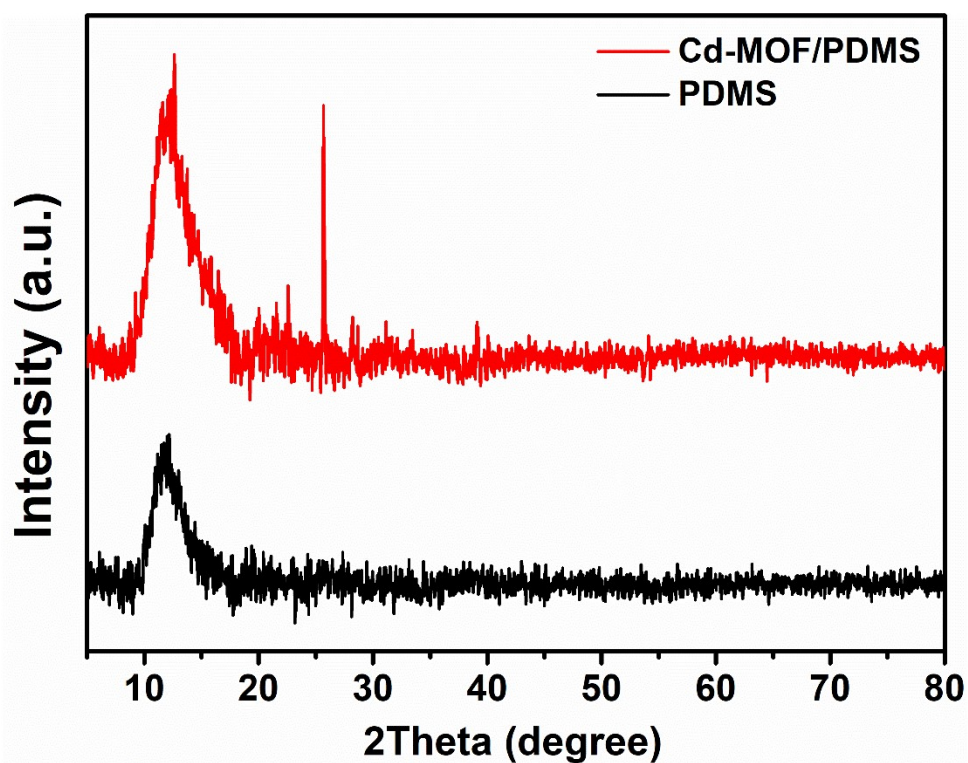


Fig S6. XRD pattern of PDMS and Cd-MOF/PDMS films.

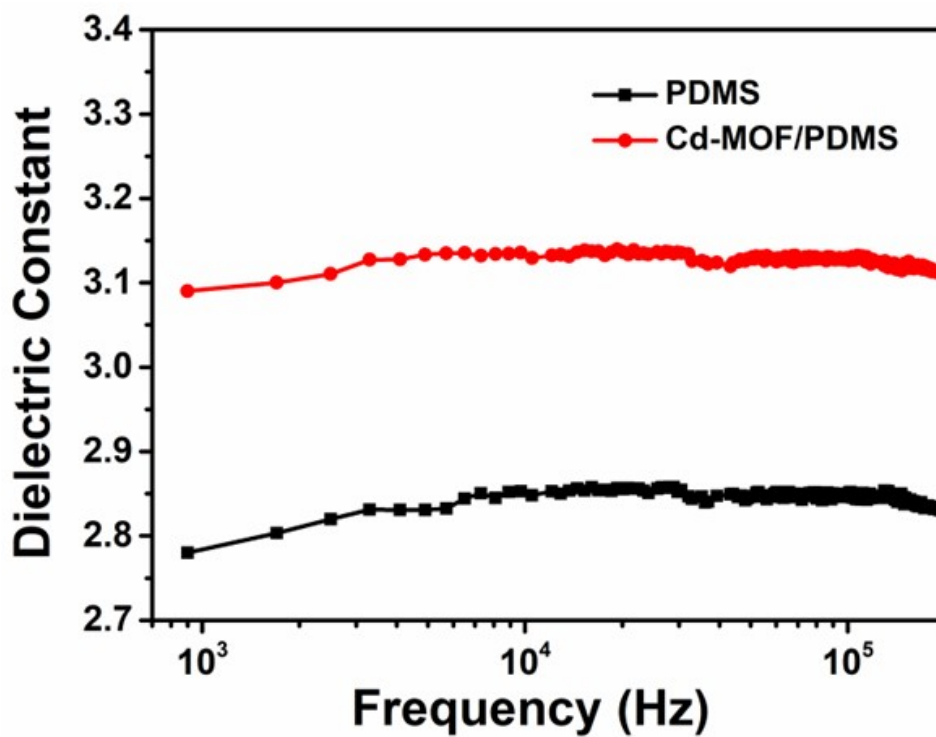


Fig S7. Dielectric constant of PDMS and Cd-MOF/PDMS films.

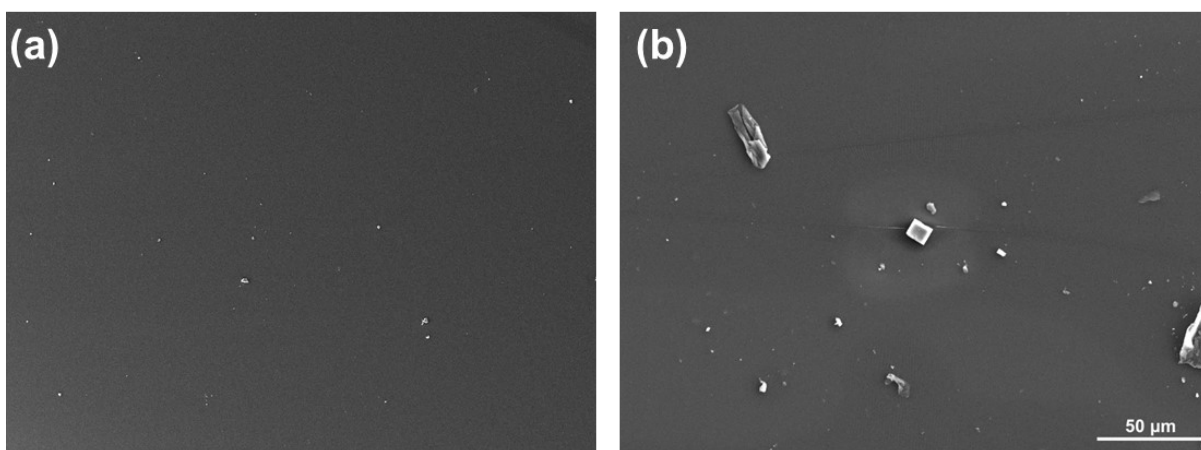


Fig S8. FE-SEM images of (a) PDMS and (b) Cd-MOF/PDMS.

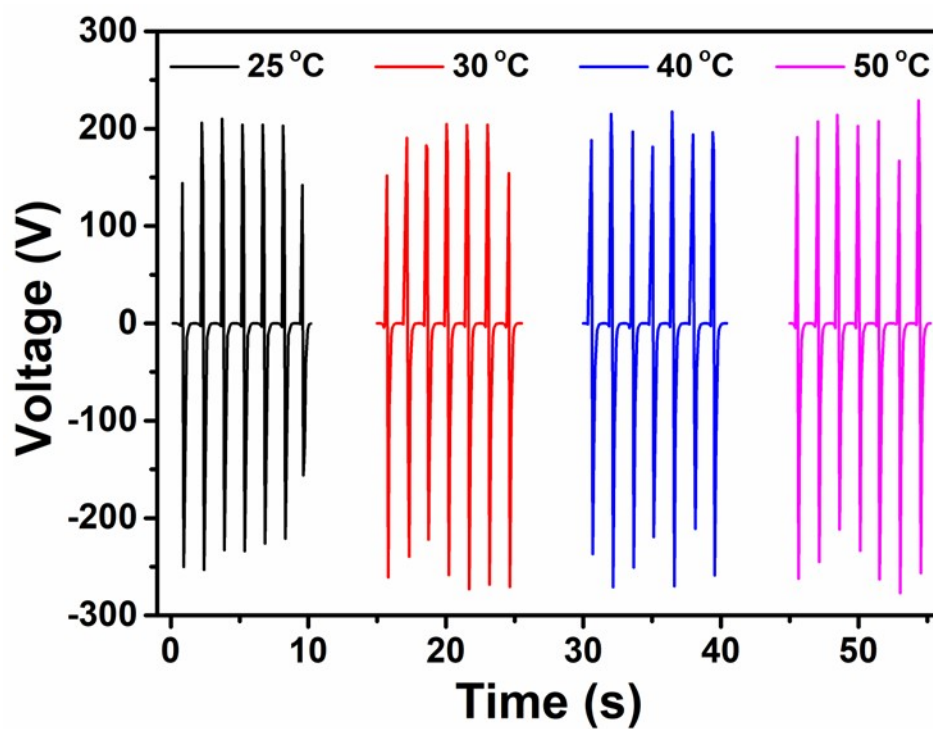


Fig S9. Output voltage under different temperature conditions from 25 °C to 50 °C.

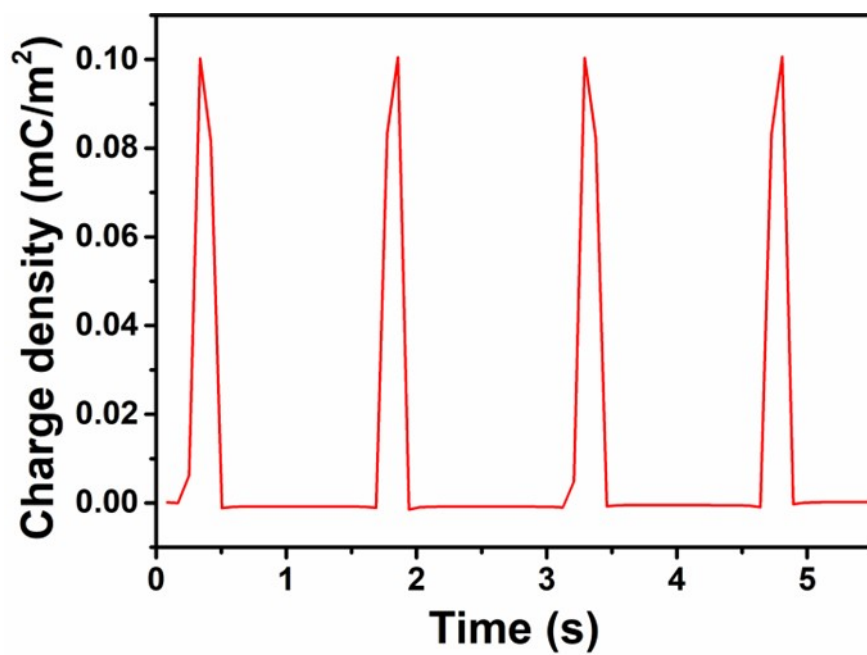


Fig S10. Output charge of the MOF-TENG.

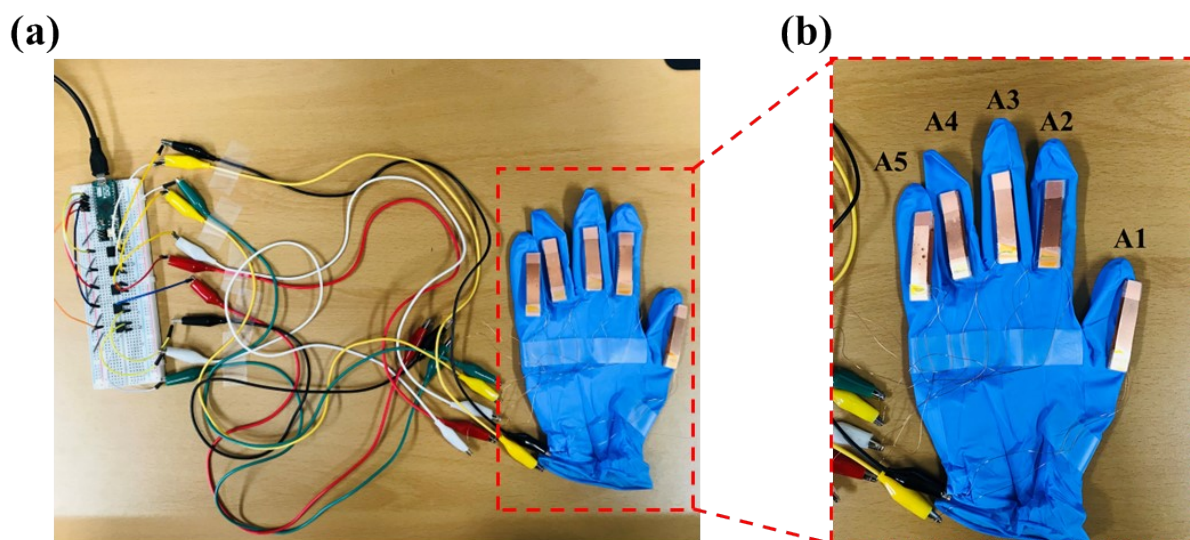


Fig S11: Digital image of (a) the air mouse setup with all the connections, (b) the glove with the MOF-TENG device attached to the fingers.

Table S1. X-ray crystal structure data and refinement parameters of Cd-MOF.

Parameters	Cd-MOF
empirical formula	C18 H14 Cd N5 O5
formula weight	492.74
crystal system	Triclinic
space group	<i>P</i> -1
<i>a</i> (Å)	7.3686(2)
<i>b</i> (Å)	9.9882(3)
<i>c</i> (Å)	13.8896(5)
α (deg)	80.054(3)
β (deg)	78.548(2)
γ (deg)	88.975(2)
wavelength (nm)	0.71073
<i>V</i> (Å ³)	986.71(5)
<i>Z</i> , <i>d</i> _{calcd} (mg m ⁻³)	2, 1.658
temperature (K)	293(2) K
θ range/deg	3.038 to 29.209 deg.
goodness-of-fit (GOOF)	1.063
<i>R</i> ₁ , <i>a wR</i> ₂ <i>b</i> [<i>I</i> > 2 σ (<i>I</i>)]	<i>R</i> ₁ = 0.0427, <i>wR</i> ₂ = 0.1113
<i>R</i> ₁ , <i>a wR</i> ₂ <i>b</i> (all data)	<i>R</i> ₁ = 0.0460, <i>wR</i> ₂ = 0.1139
absorption correction	Semi-empirical from equivalents
Limiting indices	-9 ≤ <i>h</i> ≤ 9, -13 ≤ <i>k</i> ≤ 12, -18 ≤ <i>l</i> ≤ 16
crystal size (mm ³)	0.420 x 0.230 x 0.180 mm
refinement method	Full-matrix least-squares on <i>F</i> ²
Reflections collected / unique	11056 / 4697 [<i>R</i> (int) = 0.0339]
<i>F</i> (000)	490
CCDC no.	2287569

Table S2. Selected bond lengths (Å) and bond angles (°) for Cd-MOF.

Bond Length (Å)	
Cd(1)-O(3)	2.228(2)
Cd(1)-O(1)	2.306(3)
Cd(1)-O(5)	2.309(3)
Cd(1)-N(2)	2.328(3)
Cd(1)-N(1)	2.352(3)
Cd(1)-O(2)	2.434(3)
Cd(1)-C(1)	2.720(3)
O(1)-C(1)	1.263(5)
O(2)-C(1)	1.264(5)
O(3)-C(5)	1.262(4)
O(4)-C(5)	1.237(5)
O(5)-H(5A)	0.8501
O(5)-H(5B)	0.85
N(1)-C(13)	1.323(6)
N(1)-C(9)	1.325(6)
N(2)-C(18)	1.320(6)
N(2)-C(14)	1.340(6)
N(3)-C(4)	1.334(8)
N(3)-H(3A)	0.86
N(3)-H(3B)	0.86
N(4)-C(8)	1.400(10)
N(4)-H(4A)	0.86
N(4)-H(4B)	0.8599
C(1)-C(2)	1.499(4)
C(2)-C(3)	1.384(5)
C(2)-C(4)	1.399(5)
C(3)-C(4)1	1.397(4)
C(3)-H(3)	0.93
C(5)-C(6)	1.510(5)
C(6)-C(7)	1.370(6)
C(6)-C(8)	1.404(5)

C(7)-C(8)2	1.402(5)
C(7)-H(7)	0.93
C(9)-C(10)	1.389(6)
C(9)-H(9)	0.93
C(10)-C(11)	1.374(7)
C(10)-H(10)	0.93
C(11)-C(12)	1.357(8)
C(11)-N(5)	1.454(6)
N(5)-N(5)3	1.208(8)
C(12)-C(13)	1.375(7)
C(12)-H(12)	0.93
C(13)-H(13)	0.93
C(14)-C(15)	1.362(7)
C(14)-H(14)	0.93
C(15)-C(16)	1.358(9)
C(15)-H(15)	0.93
C(16)-C(17)	1.375(9)
C(16)-N(6)	1.503(7)
N(6)-N(6)4	1.177(11)
C(17)-C(18)	1.369(7)
C(17)-H(17)	0.93
C(18)-H(18)	0.93
Bond Angle (degree)	
O(3)-Cd(1)-O(1)	120.70(11)
O(3)-Cd(1)-O(5)	87.68(10)
O(1)-Cd(1)-O(5)	91.86(11)
O(3)-Cd(1)-N(2)	93.21(12)
O(1)-Cd(1)-N(2)	145.92(12)
O(5)-Cd(1)-N(2)	92.91(11)
O(3)-Cd(1)-N(1)	89.69(11)
O(1)-Cd(1)-N(1)	90.81(12)
O(5)-Cd(1)-N(1)	176.95(10)

N(2)-Cd(1)-N(1)	85.70(12)
O(3)-Cd(1)-O(2)	170.87(10)
O(1)-Cd(1)-O(2)	55.16(10)
O(5)-Cd(1)-O(2)	84.44(10)
N(2)-Cd(1)-O(2)	91.79(11)
N(1)-Cd(1)-O(2)	98.31(11)
O(3)-Cd(1)-C(1)	147.14(12)
O(1)-Cd(1)-C(1)	27.57(11)
O(5)-Cd(1)-C(1)	86.33(10)
N(2)-Cd(1)-C(1)	119.33(12)
N(1)-Cd(1)-C(1)	96.72(11)
O(2)-Cd(1)-C(1)	27.68(11)
C(1)-O(1)-Cd(1)	94.8(2)
C(1)-O(2)-Cd(1)	88.9(2)
C(5)-O(3)-Cd(1)	127.8(2)
Cd(1)-O(5)-H(5A)	109.4
Cd(1)-O(5)-H(5B)	109.3
H(5A)-O(5)-H(5B)	104.5
C(13)-N(1)-C(9)	117.2(4)
C(13)-N(1)-Cd(1)	121.4(3)
C(9)-N(1)-Cd(1)	120.8(3)
C(18)-N(2)-C(14)	116.9(4)
C(18)-N(2)-Cd(1)	122.9(3)
C(14)-N(2)-Cd(1)	119.9(3)
C(4)-N(3)-H(3A)	120
C(4)-N(3)-H(3B)	120
H(3A)-N(3)-H(3B)	120
C(8)-N(4)-H(4A)	111.4
C(8)-N(4)-H(4B)	107.2
H(4A)-N(4)-H(4B)	109.5
O(1)-C(1)-O(2)	120.8(3)
O(1)-C(1)-C(2)	119.5(3)
O(2)-C(1)-C(2)	119.7(3)

O(1)-C(1)-Cd(1)	57.64(17)
O(2)-C(1)-Cd(1)	63.47(17)
C(2)-C(1)-Cd(1)	174.0(2)
C(3)-C(2)-C(4)	119.6(3)
C(3)-C(2)-C(1)	119.2(3)
C(4)-C(2)-C(1)	121.3(3)
C(2)-C(3)-C(4)1	122.0(3)
C(2)-C(3)-H(3)	119
C(4)1-C(3)-H(3)	119
N(3)-C(4)-C(3)1	118.2(4)
N(3)-C(4)-C(2)	123.4(4)
C(3)1-C(4)-C(2)	118.4(3)
O(4)-C(5)-O(3)	125.3(3)
O(4)-C(5)-C(6)	118.5(3)
O(3)-C(5)-C(6)	116.2(3)
C(7)-C(6)-C(8)	119.3(3)
C(7)-C(6)-C(5)	120.1(3)
C(8)-C(6)-C(5)	120.6(3)
C(6)-C(7)-C(8)2	122.2(4)
C(6)-C(7)-H(7)	118.9
C(8)2-C(7)-H(7)	118.9
N(4)-C(8)-C(7)2	117.1(5)
N(4)-C(8)-C(6)	124.3(5)
C(7)2-C(8)-C(6)	118.5(4)
N(1)-C(9)-C(10)	123.2(5)
N(1)-C(9)-H(9)	118.4
C(10)-C(9)-H(9)	118.4
C(11)-C(10)-C(9)	117.8(5)
C(11)-C(10)-H(10)	121.1
C(9)-C(10)-H(10)	121.1
C(12)-C(11)-C(10)	119.6(4)
C(12)-C(11)-N(5)	115.6(4)
C(10)-C(11)-N(5)	124.8(4)

N(5)3-N(5)-C(11)	111.7(5)
C(11)-C(12)-C(13)	118.4(5)
C(11)-C(12)-H(12)	120.8
C(13)-C(12)-H(12)	120.8
N(1)-C(13)-C(12)	123.8(5)
N(1)-C(13)-H(13)	118.1
C(12)-C(13)-H(13)	118.1
N(2)-C(14)-C(15)	123.8(5)
N(2)-C(14)-H(14)	118.1
C(15)-C(14)-H(14)	118.1
C(16)-C(15)-C(14)	118.2(5)
C(16)-C(15)-H(15)	120.9
C(14)-C(15)-H(15)	120.9
C(15)-C(16)-C(17)	119.2(5)
C(15)-C(16)-N(6)	112.4(5)
C(17)-C(16)-N(6)	128.3(6)
N(6)4-N(6)-C(16)	106.5(7)
C(18)-C(17)-C(16)	118.6(6)
C(18)-C(17)-H(17)	120.7
C(16)-C(17)-H(17)	120.7
N(2)-C(18)-C(17)	123.2(5)
N(2)-C(18)-H(18)	118.4
C(17)-C(18)-H(18)	118.4

Table S3. Comparison table for different reported MOF and COF-based TENG

Sl No	Material	Mode of TENG	Voltage	Current	Reference
1	ZIF-67 /SF	CS	118 V	8 μ A	1
2	Ni-MOF/PVDF CNF	SE	45 V	0.77 μ A	2
3	ZIF-62/Teflon	CS	62 V	1.4 μ A	3
4	MOF/SF@PDM S	CS	215 V	10 μ A	4
5	MIL-88/FEP	CS	80V	2.2 μ A	5
6	ZIF Family	CS	60 V	1.1 μ A	6
7	ZIF-67/Teflon	CS	118 V	1.7 μ A	7
8	F-COF/PVA	CS	177.8 V	26.34 mA m ⁻²	8
9	N-rich COF	CS	175V	6.3 μ A	9
10	Cd-MOF/PDMS	CS	193.4 V	0.86 μ A	This Work

References

- 1 Q. Xi, Z. Chen, Y. Li, F. Liu and Y. Guo, *ACS Appl. Electron. Mater.*, 2023, **5**, 5215–5223.
- 2 N. K. Das, M. Ravipati and S. Badhulika, *Advanced Functional Materials*, 2023, **33**, 2303288.
- 3 G. Khandelwal, N. P. M. J. Raj and S.-J. Kim, *Journal of Materials Chemistry A*, 2020, **8**, 17817–17825.
- 4 Z. Chen, Y. Cao, W. Yang, L. An, H. Fan and Y. Guo, *J. Mater. Chem. A*, 2022, **10**, 799–807.
- 5 G. Khandelwal, N. P. Maria Joseph Raj, V. Vivekananthan and S.-J. Kim, *iScience*, 2021, **24**, 102064.
- 6 G. Khandelwal, N. P. Maria Joseph Raj and S.-J. Kim, *Advanced Functional Materials*, 2020, **30**, 1910162.
- 7 S. Hajra, M. Sahu, A. M. Padhan, J. Swain, B. K. Panigrahi, H.-G. Kim, S.-W. Bang, S. Park, R. Sahu and H. J. Kim, *J. Mater. Chem. C*, 2021, **9**, 17319–17330.
- 8 L. Shi, V. S. Kale, Z. Tian, X. Xu, Y. Lei, S. Kandambeth, Y. Wang, P. T. Parvatkar, O. Shekhah, M. Eddaoudi and H. N. Alshareef, *Advanced Functional Materials*, 2023, **33**, 2212891.
- 9 S. Hajra, J. Panda, J. Swain, H.-G. Kim, M. Sahu, M. K. Rana, R. Samantaray, H. J. Kim and R. Sahu, *Nano Energy*, 2022, **101**, 107620.